Statistical and Fractal Description of Defects on Topography Surfaces

Fredrick Mwema[1*], *Tien-Chien* Jen[1]

[1]University of Johannesburg, Department of Mechanical Engineering Sciences, Auckland Park Kingsway Campus, 2006, Johannesburg, South Africa

Abstract. In this article, simulated/artificial surfaces consisting of perfectly ordered and mounded (perfect) structures and defective surfaces are characterised through statistical and fractal methods. The image sizes are designed to mimic atomic force microscopy (AFM) of scan area 1 μm^2 and maximum height features of 500 nm. The simulated images are then characterised using statistical tools such as root mean square and average roughness, skewness, kurtosis, and maximum pit and peaks. Fractal analyses are also undertaken using fractal dimensions, autocorrelation, height-height correlation and power spectral density functions. The results reveal significant differences between defective and perfectly ordered and mounded surfaces. The defective surfaces exhibit higher roughness values and lower fractal dimensions values as compared to the perfect surfaces. The results in this article can help researchers to better explain their results on topography and surface evolution of thin films.

1 Introduction

Surface topography obtained through surface imaging techniques such as atomic force microscopy (AFM) provides useful information on roughness and formation of surface morphology during surface engineering [1], [2]. In surface engineering methods such as thin film deposition, the pattern of evolution of the surface features is critical for the desired properties and performance. In fact, surface roughness characteristics of an engineered surface influences their electrical, mechanical, optical, corrosion, wear, etc. properties [3]. As such, surface roughness properties are very important for the performance of thin films. Surface roughness, literary, measures the arrangement of surface structures during a deposition process in both vertical and spatial directions. There are several tools mostly used for the characterisation of surface roughness, which are mostly classified into two categories, namely, statistical and fractal methods. Statistical analyses use tools such as average roughness, interface width, skewness, kurtosis, and maximum pit and peaks, and among other tools to compute the vertical evolution (roughness) of such surfaces [4]. On the other hand, fractal tools use methods such as fractal dimension computation, correlation functions, power spectral density function and multifractal spectrum to characterise the spatial and nanoscale

* Corresponding author: fredrick.mwema@dkut.ac.ke

dynamics of surfaces [5]. The influence of annealing on La_2O_3 thin films has been characterised by fractal and multifractal tools [6]. Fractal tools have also been used to characterise defects such as hillocks in thin films [7], [8]. The influence of the thickness of the LiF thin films evolution was studied via fractal tools [9]. The influence of the various thin film deposition conditions have been studied via fractal methods [10]–[12].

Our experience on the roughness characterisation for thin film surfaces is that there are so many inconsistences in terms of the relationship between the nature of morphology and the roughness behaviour. The question is, “can roughness characterisation be used to depict the nature of the morphology of thin films?”. It is seldom to find articles comparing the roughness properties of well-differentiated surface structures and therefore a link between morphology and roughness behaviour (vertical and lateral direction) is not strongly demonstrated in literature. In an effort to demystify the roughness characterisation (fractal), Mwema et al. [13] presented a detailed reference, which gives direction on fractal interpretation of the most common thin film surfaces. To advance knowledge and provide a further baseline on statistical and fractal interpretation of thin film surfaces, this study presents analyses and descriptions of the surface roughness (artificial topography) of perfectly ordered and mounded surfaces and a defective mounded surface with an aim of demonstrating the influence of the surface defects (such as porosity) on the statistical and fractal behaviour of thin film surfaces. The novelty of this work is that it compares the statistical and fractal properties of well-differentiated surface features with a goal to standardise the fractal descriptions of surfaces. Such comparison does not exist in published literature.

2 Methods

The topography images were designed in 3D paint tool in Microsoft OS® using primitive tools such as cylinders and spheres. The designed images were then exported to *MATLAB*® software for enhancement and calibration using tool such as *imshow, imresize, magnificationfactor,* and *imread*. The perfectly ordered and mounded surface consist of equally spaced cylindrical features (with flat tops) whereas defective image consisted of a missing number of the cylindrical features (to mimic porosity defects) as shown in Fig. 1. The images were then exported to Gwyddion® Software for statistical and fractal analyses using established standards as extensively reported in literature [14]. The procedure for analysis involved image correction using polynomial tools and flattening, computations of statistical and fractal properties using equations described in literature. The fractal tools used were fractal dimension computation, autocorrelation, height-height correlation and spectral density functions. Such tools were chosen because they are well established and have been extensively used in published articles on surface characterisations.

3 Results and Discussions

Fig. 1 shows the artificial images depicting topography of a typical surface. It shows a perfectly structured topography in 2D (Fig. 1a)) and 3D (Fig. 1b)). It also shows the same topography with a disruptive gap in 2D and 3D (Figs. 1c) and 1d)). The surface depicts a typical mounded structure of thin films or other surface engineered materials [15]. The defect in this case depicts pits, porosity, and holes on the structure of thin films [16][17], which cause disruption into the lateral patterning during deposition and growth of such structures. The scan area for the images are 1 μm^2 and the maximum height of the features are 500 nm. These are typical topography measurements for thin film surfaces using atomic force microscopy (AFM).

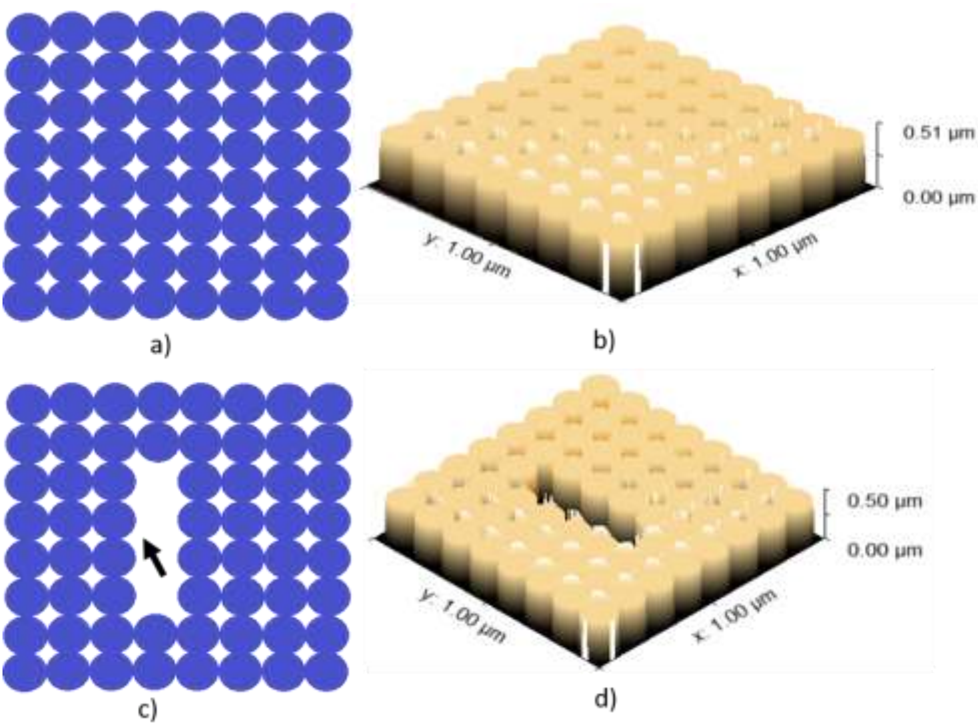

Fig. 1. Simulated images of a) 2D and b) 3D of a perfectly patterned/structured surface and c) 2D and d) 3D of the same surface with a pit defect (indicated by an arrow). The spherical structures (blue) in 2D depicts the surface grains/structures.

The line profiles for the two surfaces are shown in Fig. 2. From this analysis, the diameter of the surface grains and other features. The diameter of each grain is 0.125 nm and the interparticle distance is 0.04 nm (Fig. 2a)). The diameter of the defect in this case is 0.125 nm and length of 0.5 nm (Fig. 2b)).

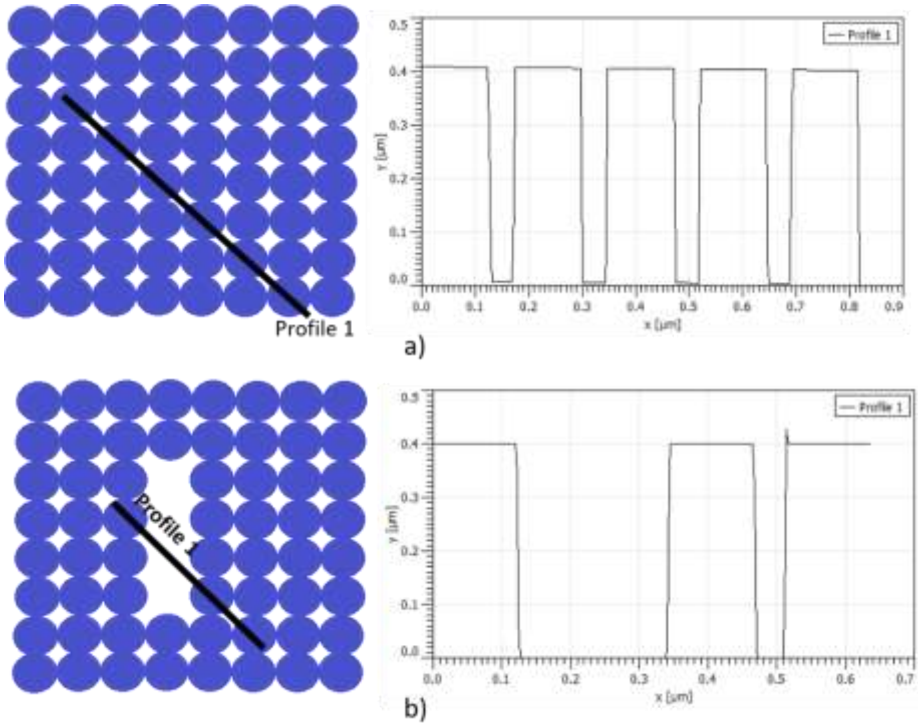

Fig. 2. Line profile analysis for the simulated images of a) a perfectly patterned/structured surface and b) a defect-containing surface.

The statistical and fractal characteristics computed for the two surfaces (i.e. perfect and defective surfaces) are represented in Table 1. The fractal dimensions were determined using four most common methods, namely, partitioning, cube counting, triangulation and power spectrum. The average values for these values are provided and computation was undertaken at a confidence level of 95%. It can be seen that the surface roughness (both root mean square and average) values for defective surfaces are higher. The presence of the defects on the surface contributes to deviation in vertical distribution of the structures and hence high surface roughness as reported in an actual thin film surface, see refs. [18], [19]. The roughness values are confirmed by the histogram for peak count versus peak height in Fig. 3. It can be seen that defective surfaces exhibit a very narrow plot as compared to perfect surface (Fig. 3). All the skewness values are negative, indicating presence of valleys; the defective skewness tends to positive, indicating growth towards asperities. The kurtosis values are smaller than 3, indicating skew towards the mean plane and stronger asperities for defective surface. The defective surfaces are seen to exhibit larger maximum peak height and smaller maximum pit depth. These parameters are used to indicate the level of valleys and deeps on the topography of surfaces respectively.

Table 1. Statistical and fractal surface roughness parameters

Surface	**Root mean square roughness (nm)**	**Average roughness (nm)**	**Maximum peak height (nm)**	**Maximum pit depth (nm)**	**Skewness**	**Kurtosis**	**Average fractal dimension**
Perfect	158.2	125.0	183.5	328.3	-1.536	0.3820	2.68 ±0.253

Defective	171.7	147.2	197.6	302.4	-1.187	-0.5765	2.60 ±0.155

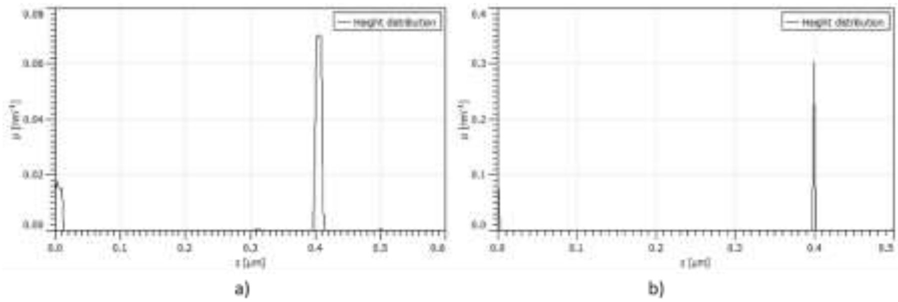

Fig. 3. The height distribution showing peak count (ρ) as a function of peak height (z) for the a) perfect and b) defective surface.

To determine the effect of the defects on the spatial roughness of thin film surfaces, fractal dimensions, autocorrelation, height-height correlation and spectral power density functions were computed and shown in table 1 and Figs. 4 and 5. The values of fractal dimension indicate strong fractal surfaces, i.e. the values are larger than 2.5. However, the average fractal dimension is higher for perfect surfaces; this indicates that defects reduce the spatial complexity of thin surfaces. The autocorrelation functions exhibit exponentially decreasing behaviour (Figs. 4 a) and b)), indicating fractal characteristics. The difference between the two functions is that the defective surfaces exhibit a steeper profile. For the height-height correlation, both surfaces are characterised by two regimes, i.e. a linear region and an oscillatory region. The oscillatory region for the perfect surface is well defined as compared to that of the defective surface. The power spectral analysis (Fig. 5) shows a clear bright central feature for the two surfaces; however, the defective surface has a clearer and larger central region, indicating the spatial features are separated from grains and defects. These observations are confirmed by the power spectral density functions (Fig. 5).

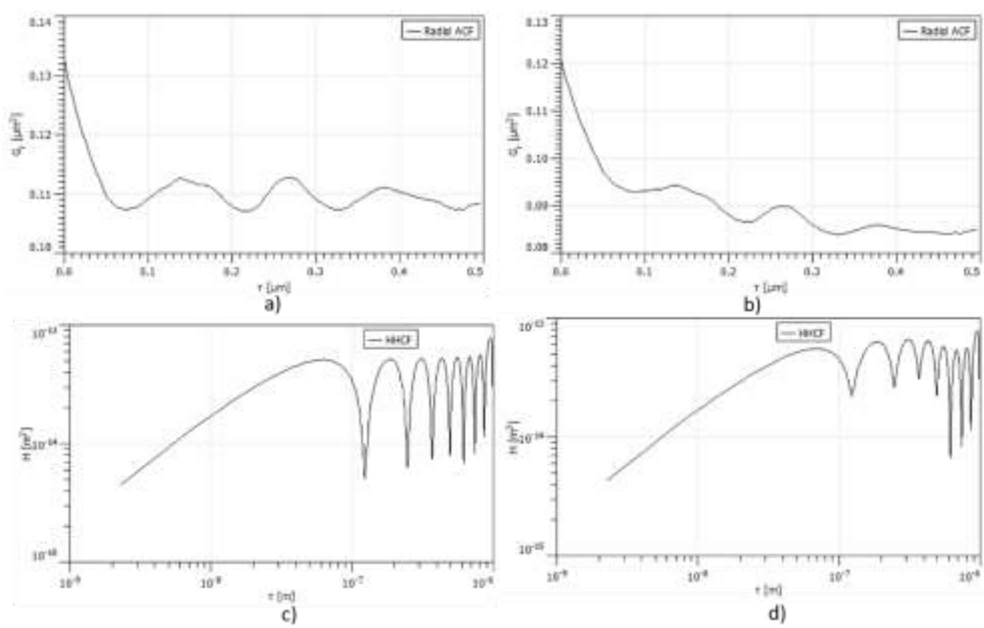

 https://doi.org/10.1051/matecconf/202337401001

Fig. 4. Autocorrelation functions for a) perfect and b) defective surfaces and height-height correlation functions for c) perfect and b) defective surfaces.

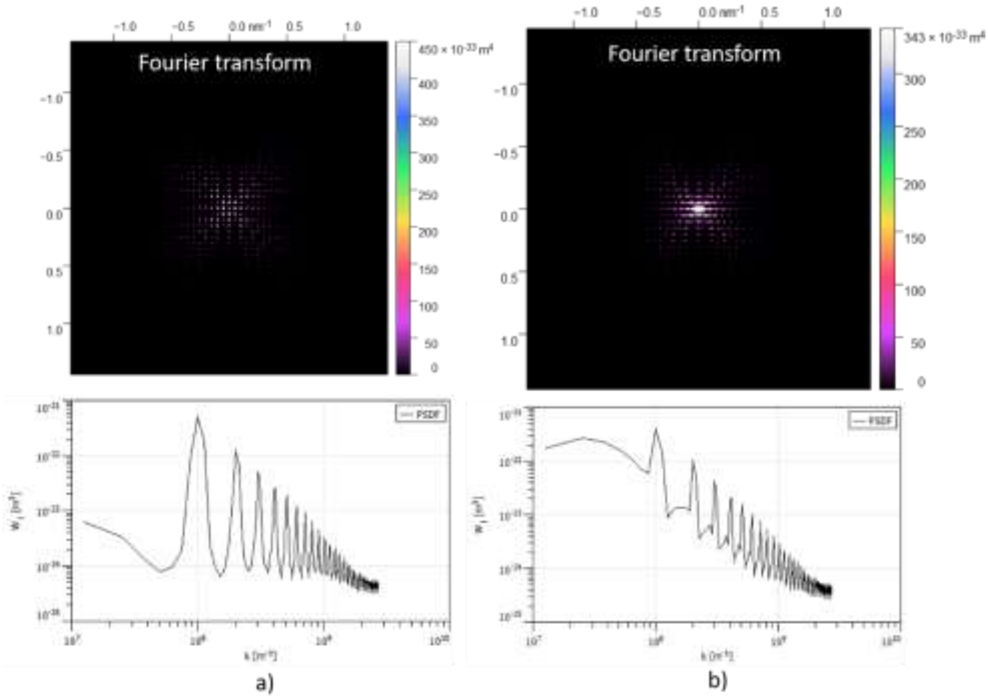

Fig. 5. Fourier transform power spectrum and corresponding spectral power density functions for a) perfect and b) defective surfaces

4 Conclusions

In this article, artificially created topography images of scan size of 1 μm × 1 μm and with maximum height of features of 500 nm have been analysed. One surface exhibited a perfect (ordered) arrangement of surface grains whereas the other surface exhibited defects (in terms of porosity). The surfaces were analysed for statistical and fractal characteristics to understand the ideal influence of defects on these properties. The key conclusions from the analysis are listed:

a) The root mean square roughness and average roughness for the defect surface was shown to be higher than the perfect/ordered surface.
b) The defective surface had the smallest negative value of skewness and smaller value of kurtosis.
c) The fractal dimension for defective surfaces is smaller than that of the perfectly ordered surface.
d) The autocorrelation function for defective surface is steeper than that of the perfectly ordered surface.
e) The power spectrum (Fourier transforms) indicates that the central region of defective surfaces is larger and brighter than that of the perfectly ordered surface.

This study shall be useful in demystifying the statistical and fractal description of actual topography images (obtained via AFM, STM, etc.). Researchers in surface engineering can utilise this work in describing the surface properties of topography images obtained from actual surfaces. The future prospect of the area is to carry out an analysis with more defective images and compare with images of actual surfaces.

References

[1] Ş. Ţălu, S. Stach, V. Sueiras, and N. M. Ziebarth, “Fractal Analysis of AFM Images of the Surface of Bowman’s Membrane of the Human Cornea,” *Ann. Biomed. Eng.*, vol. 43, no. 4, pp. 906–916, 2015, doi: 10.1007/s10439-014-1140-3.

[2] Ş. Ţălu, M. Bramowicz, S. Kulesza, and S. Solaymani, “Topographic characterization of thin film field-effect transistors of 2,6-diphenyl anthracene (DPA) by fractal and AFM analysis,” *Mater. Sci. Semicond. Process.*, vol. 79, no. February, pp. 144–152, 2018, doi: 10.1016/j.mssp.2018.02.008.

[3] F. H. Wang and C. L. Chang, “Effect of substrate temperature on transparent conducting Al and F co-doped ZnO thin films prepared by rf magnetron sputtering,” *Appl. Surf. Sci.*, vol. 370, pp. 83–91, 2016, doi: 10.1016/j.apsusc.2016.02.161.

[4] E. S. Gadelmawla, M. M. Koura, T. M. A. Maksoud, I. M. Elewa, and H. H. Soliman, “Roughness parameters,” *J. Mater. Process. Technol.*, vol. 123, no. 1, pp. 133–145, 2002, doi: 10.1016/S0924-0136(02)00060-2.

[5] F. M. Mwema, E. T. Akinlabi, and O. P. Oladijo, *Sputtered Thin Films: Theory and Fractal Descriptions*. CRC Press, 2021.

[6] G. Liu, L. Wu, and F. Zhang, “Multifractal spectra of atomic force microscope images of lanthanum oxide thin films deposited by electron beam evaporation,” *Mater. Sci. Semicond. Process.*, vol. 31, pp. 14–18, Mar. 2015, doi: 10.1016/j.mssp.2014.11.011.

[7] F. M. Mwema, E. T. Akinlabi, and O. P. Oladijo, “Fractal analysis of hillocks: A case of RF sputtered aluminum thin films,” *Appl. Surf. Sci.*, vol. 489, pp. 614–623, Sep. 2019, doi: 10.1016/j.apsusc.2019.05.340.

[8] S. Nazarpour and M. Chaker, “Fractal analysis of Palladium hillocks generated due to oxide formation,” *Surf. Coatings Technol.*, vol. 206, no. 11–12, pp. 2991–2997, 2012, doi: 10.1016/j.surfcoat.2011.12.036.

[9] R. P. Yadav, S. Dwivedi, A. K. Mittal, M. Kumar, and A. C. Pandey, “Fractal and multifractal analysis of LiF thin film surface,” *Appl. Surf. Sci.*, vol. 261, pp. 547–553, 2012, doi: 10.1016/j.apsusc.2012.08.053.

[10] A. V. Dvornichenko and V. O. Kharchenko, “Scaling properties of the growing monolayer on the disordered substrate,” *Phys. Lett. A*, vol. 384, no. 16, p. 126329, Jun. 2020, doi: 10.1016/j.physleta.2020.126329.

[11] L. Zuo, D. Zuo, Y. Zhu, and H. Wang, “Effect of process parameters on surface topography of friction stir welding,” *Int. J. Adv. Manuf. Technol.*, vol. 98, no. 5–8, pp. 1807–1816, Sep. 2018, doi: 10.1007/s00170-018-2326-x.

[12] Ş. Ţălu *et al.*, “Micromorphology analysis of specific 3-D surface texture of silver chiral nanoflower sculptured structures,” *J. Ind. Eng. Chem.*, vol. 43, pp. 164–169, 2016, doi: 10.1016/j.jiec.2016.08.003.

[13] F. M. Mwema, E. T. Akinlabi, and O. P. Oladijo, *Demystifying Fractal Analysis of Thin Films: A Reference for Thin Film Deposition Processes*. 2021.

[14] Ş. Ţălu, S. Stach, D. Raoufi, and F. Hosseinpanahi, “Film thickness effect on fractality of tin-doped In2O3 thin films,” *Electron. Mater. Lett.*, vol. 11, no. 5, pp. 749–757, Sep. 2015, doi: 10.1007/s13391-015-4280-1.

[15] D. Siniscalco, M. Edely, J. F. Bardeau, and N. Delorme, “Statistical analysis of mounded surfaces: Application to the evolution of ultrathin gold film morphology

with deposition temperature," *Langmuir*, vol. 29, no. 2, pp. 717–726, 2013, doi: 10.1021/la304621k.

[16] E. Ji, C. Cummins, and G. Fleury, "Precise synthesis and thin film self-assembly of PLLA-b-PS bottlebrush block copolymers," *Molecules*, vol. 26, no. 5, 2021, doi: 10.3390/molecules26051412.

[17] F. Alfeel, F. Awad, I. Alghoraibi, and F. Qamar, "Using AFM to Determine the Porosity in Porous Silicon," *J. Mater. Sci. Eng. A*, vol. 2, no. 9, pp. 579–583, 2012.

[18] D. Q. Tan, "Differentiation of roughness and surface defect impact on dielectric strength of polymeric thin films," *IET Nanodielectrics*, vol. 3, no. 1, pp. 28–31, Mar. 2020, doi: 10.1049/iet-nde.2019.0031.

[19] J. L. Clabel H. *et al.*, "Growth process and grain boundary defects in Er doped BaTiO3 processed by EB-PVD: A study by XRD, FTIR, SEM and AFM," *Appl. Surf. Sci.*, vol. 493, no. July, pp. 982–993, Nov. 2019, doi: 10.1016/j.apsusc.2019.07.003.